Light Metals 2012 *Edited by: Carlos E. Suarez*
TMS (The Minerals, Metals & Materials Society), 2012

THE USE OF VORTEX METHOD IN THE ANALYSIS OF MULTIPHASE FLOW IN ALUMINUM REDUCTION CELLS

ZHANG Hehui, ZHANG Hongliang, LI Jie, XU Yujie, YANG Shuai, LAI Yanqing

School of Metallurgical Science and Engineering, Central South University, Changsha, Hunan, 410083, P.R.China

Keywords: aluminum reduction cell; vortex; vorticity; swirling strength; computational fluid dynamics

Abstract

As the principal character of flow pattern, the vortex distribution plays a dominant role in the flow behavior of aluminum reduction cells, thereby affecting the cell performance. Based on the commercial CFD software CFX12, the method of vorticity and swirling strength was introduced to analyze vortex structures of the bath and metal phases quantificationally in a 300 kA cell, in which both the influences of electromagnetic forces (EMFs) and gas bubbles were included. Research results prove that, compared with velocity vector distribution and streamline picture, it can provide more flow field information with the above method, which may help to the optimization of alumina feeding points configuration. Vortexes usually occur as reverse symmetrical pairs. The single factor comparative study shows that the EMFs tend to trigger large vortexes near the upstream side, while gas bubbles mainly stir the bath and generate small ones around anodes.

Introduction

It is well known that the melt flow in aluminum reduction cells is turbulent flow [1], in which there exist vortexes mainly circulated by gas bubbles and electromagnetic forces (EMFs). The flow pattern characterized by vortex distribution is very important because it is connected closely to the cell performance. Sun *et al.* [2] studied the effect of background melt flows and interface deformation on stability characteristics of the cell, using the linear stability analysis method. They concluded that the melt flow with 3 vortexes is more stable than others. Antille *et al.* [3] have found that the symmetry of the vortexes decreases under abnormal operation after model calculation and real measurements, which is due to the fluctuations of current. In a US patent [4], Brown affirmed that by improving the wettability between molten aluminum and cathode carbon, the vortex strength would be lower and the anode cathode distance (ACD) can also be reduced.

Owing to the importance of vortex distribution, it becomes the focus of the computational fluid dynamics (CFD) studies of the cell. However, for most references, the description of vortex is made from the velocity vector diagram. In this way, the size and direction of vortex is roughly estimated by observing the velocity vectors structure, which is often unavoidably subjective. Besides, information about the strength and rotation speed of vortex is not available in that diagram. Therefore, to mine and process more flow field information, a new method of analyzing the vortex distribution needs to be put forward.

This paper firstly gives an inhomogeneous three-phase model for the flow in a 300 kA pre-baked anode cell based on the commercial CFD code CFX 12.0, in which the effect of EMFs was included. Then, with an exact prediction of both the metal and bath flow field, the method of vorticity and swirling strength was introduced to analyze vortex structures of the bath and metal phases quantificationally and obtain more substantial fluid information. At last, the influence of gas bubbles and EMFs on the vortex structures in bath was discussed respectively to briefly explore the formation mechanism of vortexes.

Model description

Three-phase model

In this article, the fluid system consisting of bath, metal and anode gas in a full 300 kA aluminum reduction cell with 20×2 prebaked anodes was studied as an application case. The three-phase flow in the cell was computed based on the Euler/Euler approach by solving the time-averaged Navier-Stokes equations to get the steady state flow condition, where the influences of alumina particles and heat transfer were neglected. Thus, the inhomogeneous equations for conservation of mass and momentum can be written as follows:

$$\frac{\partial}{\partial t}\left(r_\alpha \rho_\alpha\right)+\nabla\cdot\left(r_\alpha \rho_\alpha \boldsymbol{U}_\alpha\right)=0 \tag{1}$$

$$\frac{\partial}{\partial t}\left(r_\alpha \rho_\alpha \boldsymbol{U}_\alpha\right)+\nabla\cdot\left[r_\alpha\left(\rho_\alpha \boldsymbol{U}_\alpha\times\boldsymbol{U}_\alpha\right)\right]$$
$$=-r_\alpha\nabla p_\alpha+\nabla\cdot\left\{r_\alpha\mu_{\alpha eff}\left[\nabla\boldsymbol{U}_\alpha+\left(\nabla\boldsymbol{U}_\alpha\right)^T\right]\right\}+\boldsymbol{S}_{M\alpha}+\boldsymbol{M}_\alpha \tag{2}$$

Where r_α, ρ_α, $\boldsymbol{U}_\alpha$, P_α and $\mu_{\alpha eff}$ are volume fraction, density, velocity, pressure and effective viscosity of phase α respectively.

The EMFs were treated as the momentum source term $\boldsymbol{S}_{M\alpha}$ all over the fluid domain, which could be calculated from the cross product of electric current density and magnetic induction intensity. For the interfacial forces $\boldsymbol{M}_\alpha$, only the interphase drag force induced by gas bubble was considered. The details for the modeling and solving of the three-phase flow can be found in our previous work [5].

The analysis method of vortex

It is the rotating speed and swirling strength that constitute the main features of vortex, and both of them can be represented mathematically by the method of vorticity and swirling strength respectively based on the flow field calculation results.

The vorticity, namely the curl of velocity field, is twice as the rotating speed of fluid:

$$\boldsymbol{\Omega}=2\boldsymbol{\omega}=\nabla\times\boldsymbol{U} \tag{3}$$

Where,

$\boldsymbol{\Omega}$: Vorticity, s^{-1}

$\boldsymbol{\omega}$: Angular velocity, s^{-1}

U : Fluid velocity

The vorticity is a vector, and the direction of it can be judged by the right-hand rule: curl the fingers of the right hand into a fist and keep the thumb out, then match the fingers curl in to the moving way of the fluid and the thumb will point to the vorticity direction.

For the convenience of analysis, a cross section is often selected from the whole fluid domain. In this case, the components of vorticity in three directions need to be calculated as follows:

$$\Omega_x = \frac{\partial w}{\partial y} - \frac{\partial v}{\partial z} \tag{4}$$

$$\Omega_y = \frac{\partial u}{\partial z} - \frac{\partial w}{\partial x} \tag{5}$$

$$\Omega_z = \frac{\partial v}{\partial x} - \frac{\partial u}{\partial y} \tag{6}$$

Where u, v, w are the components of velocity in the x, y, z directions respectively.

The tensor of local velocity field can be written as:

$$\boldsymbol{D} = \begin{bmatrix} \frac{\partial u}{\partial x} & \frac{\partial u}{\partial y} & \frac{\partial u}{\partial z} \\ \frac{\partial v}{\partial x} & \frac{\partial v}{\partial y} & \frac{\partial v}{\partial z} \\ \frac{\partial w}{\partial z} & \frac{\partial w}{\partial z} & \frac{\partial w}{\partial z} \end{bmatrix} \tag{7}$$

Zhou *et al.* [6, 7] proposed that the imaginary part of plural eigenvalue of the above tensor could be taken to quantify the strength of vortex, which it was called swirling strength. As a mathematical tool to measure the strength of vortex, the higher the local swirling strength is, the stronger the fluid vortex is. If the local swirling strength is close to zero, there does not exit any vortex motion. The measurement and analysis results of turbulent flow made by Adrian *et al.* [8] have proved the validity of this method.

Results and discussion

Vortex distribution of bath

At first, the bath flow is taken as an example to illustrate how the vortex analysis method makes a difference in the information processing of velocity field, with the consideration of its high complexity [9]. The overall sense of the vortex distribution can be obtained by examining contour maps of the swirling strength and vorticity on the interpolar horizontal plane of bath in Fig. 1, where the common displaying method of flow field known as velocity vectors and streamlines is also taken for comparison.

It is obvious to see that the vortex analysis method can give the vortex information more impersonally and accurately compared with the ways of velocity and streamlines. Particularly, with the swirling strength method, it is clear to observe the influence range and strength of vortexes in Fig. 1a, where only the area with colored contour exits recognizable vortex motion. However, as most velocity vectors and streamlines are complex and disordered, different observer may get different opinions about the vortex structures by observing the vectors and streamlines, let alone judging the exact vortex size.

Meanwhile, only with the contour map of vorticity (Fig. 1b), can the distribution of rotation speed be obtained exactly, which is closely interrelated with the material transportation. Generally, vortexes in bath usually occur as reverse symmetrical pairs, namely the vorticity of the adjacent or symmetrical vortex pairs is approximately equal and opposite.

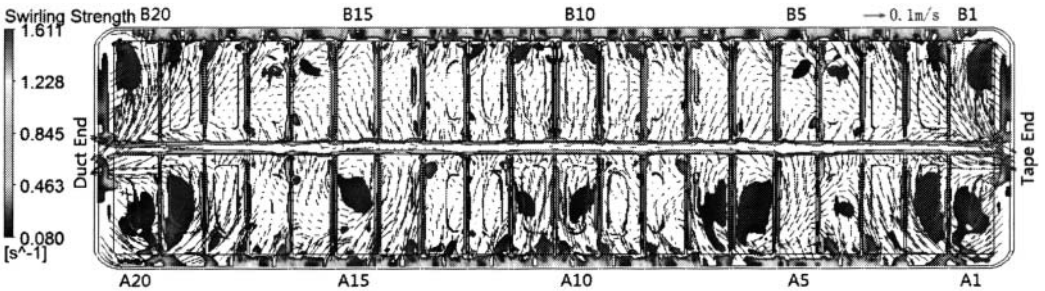

(a) Contour map of swirling strength and velocity vectors

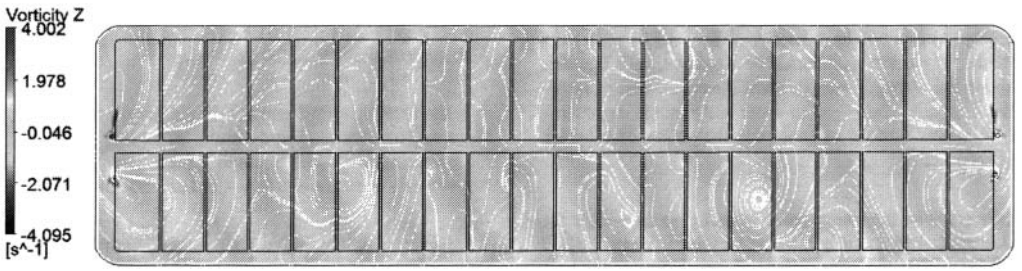

(b) Contour map of vorticity and streamlines

Fig. 1 Flow field on the interpolar horizontal plane of bath

Influences of gas bubble and EMFs on the formation of vortexes in bath

In order to investigate the effect of gas bubbles and EMFs on the formation of vortexes in bath, contrastive studies are made where the bath melt is driven by different kinds of forces, i.e. anode gas only, EMFs only and both of the above two forces. The maximum and average values of the absolute vorticity and swirling strength under different affecting factors are shown in Table 1.

The data in table 1 explains that both gas bubbles and EMFs have some influences on the formation of vortexes, and their combined action will enhance the rotation speed and strength of vortexes.

However, their function characteristics are very different. In particular, the contour map of swirling strength under the action of EMFs is shown in Fig. 2. In Fig. 1, the regions of high swirling strength are located in the anode slots. But in Fig. 2, there are few vortexes in that area, which reveals that the circulation of gas contributes to the formation of small vortexes around the anode slots.

Similar to Fig. 1a, in Fig. 2, instead of uniform distributing, the vortexes near the upstream side (Side A in Fig. 1a) are stronger than that near the downstream side (Side B). And there are obvious vortex motion under the anodes close to the riser bus bar such as the anode numbered with A1-A2, A6-A7, A10-A12, A15 and A19-A20. The reason of the asymmetry of vortex structure is that the EMFs are usually not uniformly distributed.

The distribution of EMFs is shown in Fig. 3, in which the force vectors are deflected along the short axis of the cell, and the EMFs near the upstream side are significantly greater than those near the downstream side.

Table 1 Maximum and average values of the absolute vorticity and swirling strength under different affecting factors

Effector factor	Absolute vorticity		Swirling strength	
	$\lvert\Omega_Z\rvert_{max}$ / s^{-1}	$\lvert\Omega_Z\rvert_{ave}$ / s^{-1}	$\lambda_{ci\ max}$ / s^{-1}	$\lambda_{ci\ ave}$ / s^{-1}
Both anode gas and EMFs	4.095	0.200	1.611	0.097
Anode gas only	1.602	0.141	1.365	0.091
EMFs only	1.620	0.153	1.103	0.070

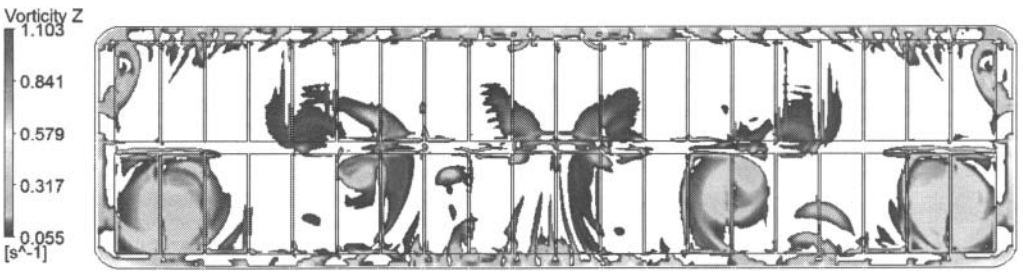

Fig. 2 Contour map of swirling strength on interpolar horizontal plane under the action of EMFs

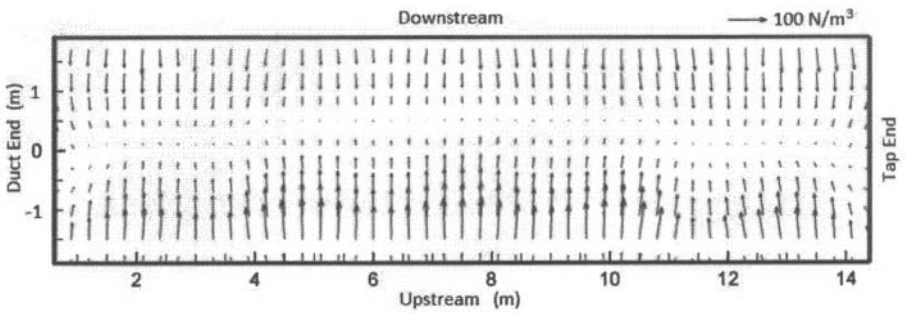

Fig. 3 Vectors of electromagnetic force on the interpolar horizontal plane

Vortex distribution of metal

The contour maps of swirling strength and vorticity of metal are shown in Fig. 4 and Fig. 5 respectively. Compared with bath, the size of vortexes in metal is generally larger, but the maximum values of swirling strength and vorticity are much smaller (compare Fig. 1, Fig. 4 and Fig. 5). This is because the buoyancy effect of anode bubble on the metal is very limited, so the EMFs dominate the vortex motion of metal without the violent stirring of bubble gas near the anode slots.

Due to the ignorable negative pressure effect caused by vortexes, the interface shape of bath and metal may depends on the vortex structure. Thus, it may be helpful for the reducing of ACD if a stable and uniform distribution of vortex is maintained.

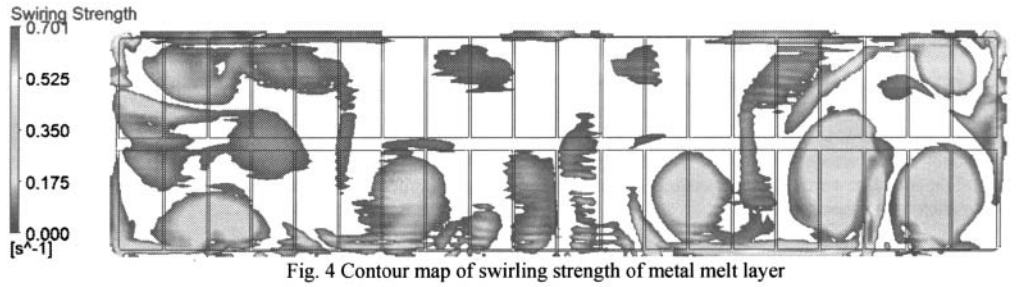

Fig. 4 Contour map of swirling strength of metal melt layer

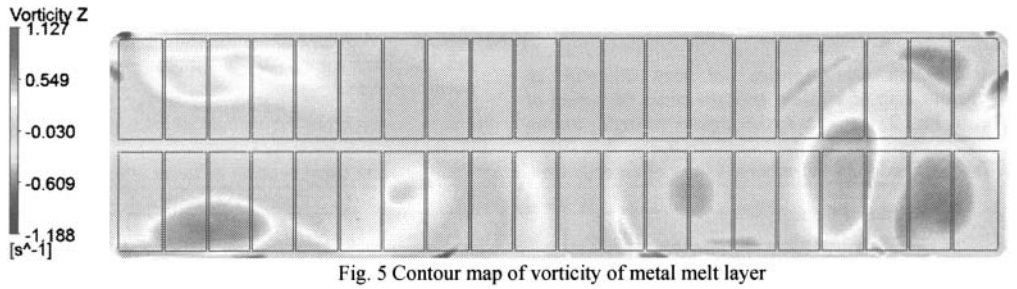

Fig. 5 Contour map of vorticity of metal melt layer

Guidance for the alumina feeder locations

The select of location of alumina feeders has been proved very important, because the mixing effect of alumina depends strongly on the local flowing of bath [10]. The contour map of vorticity distribution on horizontal plane above anode bottom is shown in Fig. 6.

For large-scale aluminum reduction cell, the alumina feeders are usually equally located in the center channel. There are four small reverse symmetrical vortexes with high vorticity around each intersection of anode slots and center channel. If the alumina feeder is set there, alumina piles made of particles may be crushed immediately and then scattered quickly. This deduction agrees with the experimental result of Chesonis *et al.* [11]. While, to select several specific feeder points from all the junctures of the small channels and the center channel to make the most suitable feeder configuration, a follow-up study remains to be made.

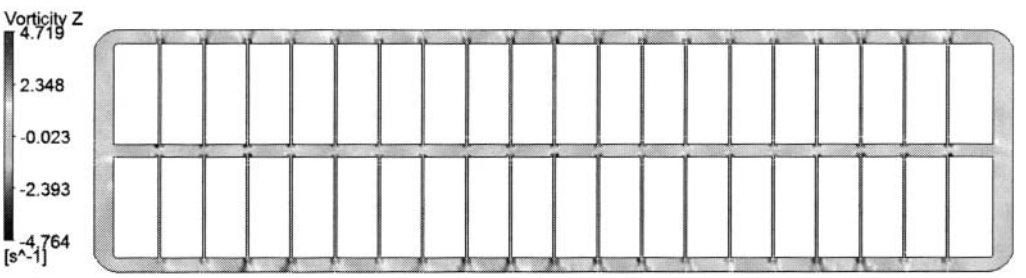

Fig. 6 Contour map of vorticity distribution on horizontal plane above anode bottom

Conclusions

This paper demonstrates the effectiveness of vortex method in the processing and analyzing of flow field information for the CFD studying in aluminum reduction cells. Although the flow structure in the cell is very complex with abundant vortexes signifying violent turbulence, the vortex structure can be described quantificationally and clearly with the method of swirling strength and vorticity. So the above method is a complement to the way of velocity vectors and streamlines in the processing of flow field in the cells.

Vortexes in the cell usually occur as reverse symmetrical pairs drived by EMFs and gas bubbles. Between them, EMFs tend to trigger large vortexes near the upstream side in both metal and bath, while gas bubbles mainly stir the bath and generate small ones around anodes.

As more flow field information can be obtained in a precise and relatively straight way with this method, it may be helpful to use it to guide and evaluate the industrial practice such as the optimizing of EMFs distribution and alumina feeders placement.

Acknowledgements

The authors are grateful for the financial support of the National Natural Science Foundation of China (51104187) and the Research Fund for the Doctoral Program of Higher Education in China (20100162120008).

References

[1] Ai D K. Hydrodynamics of the Hall-Héroult cell. In Bohner H O, eds. Light Metals 1985. New York, NY: The Metallurgical Society of AIME, 1985. 593-607.

[2] Sun H, Oleg Z, Bruce A F, Donald P Z. The influence of the basic flow and interface deformation on stability of Hall-Héroult cells. In Kvande H, eds. Light Metals 2005. San Francisco, CA: TMS (The Miners, Metals & Materials Society), 2005: 437–441.

[3] Antille J, Kaenel R. Using a magnetohydrodynamic model to analyze pot stability in order to indentify an abnormal operating condition. In Schneider W, eds. Light Metals 2002. Columbus, GA: TMS (The Miners, Metals & Materials Society), 2002: 73–78.

[4] Brown C W. Cathode for a Hall-Heroult type electrolytic cell for producing Aluminum: USA, 20030196908A1 [P]. Oct. 23, 2003.

[5] LI Jie, XU Yu-jie, ZHANG Hong-liang, LAI Yan-qing. An inhomogeneous three-phase model for the flow in aluminium reduction cells. International Journal of Multiphase Flow, 2011, 37(1): 46–54.

[6] Zhou J, Adrian R J, Balachandar S. Autogeneration of near-wall vortical structures in channel flow. Physics of Fluids, 1996, 8 (1): 288–290.

[7] Zhou J, Adrian R J, Balachandar S, Kendally T M. Mechanisms for generating coherent packets of hairpin vortices in channel flow. J. Fluid Mech, 1999, 387: 353–396.

[8] Adrian R J, Christensen K T, Liu Z C. Analysis and interpretation of instantaneous turbulent velocity fields. Experiments in Fluids, 2000, 29 (3): 275–290.

[9] Feng Y Q, Cooksey M, Schwarz M P. CFD modeling of electrolyte flow in aluminium reduction cells. In: Sørlie M, eds. Light Metals 2007. Orlando, FL: TMS (The Miners, Metals & Materials Society), 2007: 339–344.

[10] Feng Y Q, Cooksey M A, Schwarz M P. CFD modeling of alumina mixing in aluminium reduction cells. In: Lindsay J, eds. Light Metals 2011. San Diego, CA: TMS (The Minerals, Metals & Materials Society), 2011: 543-548.

[11] Chesonis D C, Johansen S T, Rolseth S, Thonstad J. Gas induced bath circulation in aluminium reduction cells. Journal of Applied Electrochemistry, 1989, 19 (5): 703–712.